All-Energy Search for Solar Atmospheric Neutrinos with IceCube

The IceCube Collaboration

(a complete list of authors can be found at the end of the proceedings)

E-mail: jlazar@icecube.wisc.edu, imartinezsoler@g.harvard.edu

The interaction of cosmic rays with the solar atmosphere generates a secondary flux of mesons that decay into photons and neutrinos – the so-called solar atmospheric flux. Although the gamma-ray component of this flux has been observed in Fermi-LAT and HAWC Observatory data, the neutrino component remains undetected. The energy distribution of those neutrinos follows a soft spectrum that extends from the GeV to the multi-TeV range, making large Cherenkov neutrino telescopes a suitable for probing this flux. In this contribution, we will discuss current progress of a search for the solar neutrino flux by the IceCube Neutrino Observatory using all available data since 2011. Compared to the previous analysis which considered only high-energy muon neutrino tracks, we will additionally consider events produced by all flavors of neutrinos down to GeV-scale energies. These new events should improve our analysis sensitivity since the flux falls quickly with energy. Determining the magnitude of the neutrino flux is essential, since it is an irreducible background to indirect solar dark matter searches.

Corresponding authors: Jeff Lazar[1,2*], Ivan Martinez-Soler[2]

[1] *Department of Physics and Laboratory for Particle Physics and Cosmology, Cambridge 02138, MA, United States*

[2] *Department of Physics and Wisconsin IceCube Particle Astrophysics Center University of Wisconsin–Madison, Madison 53703, WI, United States*

* Presenter

ICRC2023
38th International Cosmic Ray Conference
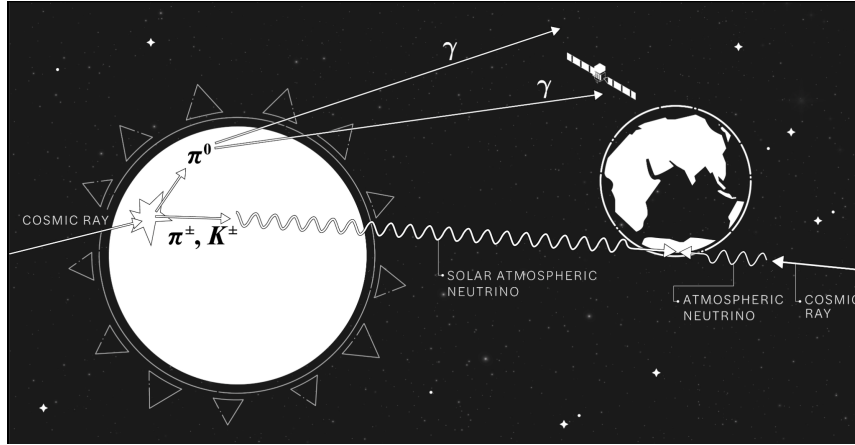The Astroparticle Physics Conference

Figure 1: Description of the solar atmospheric flux neutrino production by the collision of the cosmic ray flux with the solar atmosphere. Together with the neutrino flux, a high-energy gamma ray flux is also created.

1. Introduction

The Sun is a non-stopping source of neutrinos. At the MeV scale, a flux of electron neutrinos is produced in the thermonuclear reactions happening in the solar core. Two processes take place, *pp* chains and CNO cycle [1], creating a neutrino flux that extends up to ~ 20 MeV. The weak neutrino cross section, allows them to escape from the Sun and reach the Earth. The first observation of the solar neutrino flux was done in Homestake experiment [2].

In addition to nuclear reactions, other processes that take place in the Sun also creates a neutrino flux. At energies above the MeV scale, the interaction of the cosmic ray flux with the solar atmosphere generates a secondary flux of mesons and muons, and its decay creates a neutrino flux. Like the atmospheric neutrino flux created in the Earth's atmosphere, this flux extends for seven others of magnitude in energy, from ~ 10 MeV to ~ 100 TeV, making that flux accesible to neutrino telescope experiments. In Figure 1, we have a schematic description of the solar atmospheric neutrino flux production.

The neutral mesons decay, also produced in the cosmic ray interactions, leads to a high energy photon flux that has been measured up to ~ 200 GeV. This energetic photon flux has already been observed by Fermi-LAT [3] and HAWC [4] showing large discrepancies with the predicted flux. The gamma ray spectrum shows a deep at energies close to ~ 50 GeV. The detection of the neutrino flux produced with those photons will provide complementary information about the cosmic ray interaction with the Sun, which can shed light over the anisotropies over the observed flux.

Additionally, the scattering of Dark Matter (DM) with the nucleons will accumulate DM inside the Sun due to the loss of its kinetic energy after the scattering with the Sun nuclei. Different DM annihilation channels can produce a multi-GeV neutrino flux in the Sun. Therefore, knowing the solar atmospheric neutrinos is important since they are a background in DM searches.
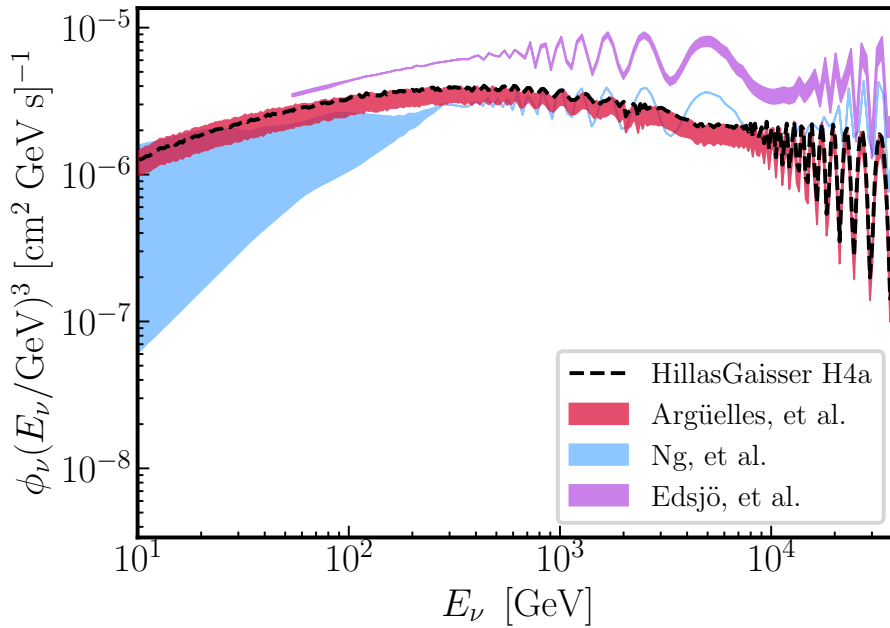
Figure 2: *Expected solar atmospheric flux at the Earth surface.* Several groups have estimated the solar atmospheric neutrino flux and its uncertainties based on the different cosmic ray models, hadronic interactions, and the impact of the solar magnetic field over cosmic ray propagation. In this plot, we show the results from three different groups.

2. Flux Expectation

The interaction of the cosmic-ray flux with the solar atmosphere produces a flux of mesons, comprised mainly of $\pi^{\pm}$, π^0, $K^{\pm}$, and K^0 mesons, with a small contribution from D mesons. The subsequent decay of the charged mesons gives rise to a flux of neutrinos, either directly or through μ decay. This is the same process that gives rise to the terrestrial atmospheric flux; however, since the solar atmosphere is less dense than that of the Earth, the intermediate mesons and μ undergo fewer interactions and thus lose less energy. Therefore, the solar flux follows a slightly harder spectrum than its earthly counterpart. It should be noted, however, that this flux is still quickly falling relative to the astrophysical neutrino spectrum. After crossing the Sun's surface, the mesons lose their energy in the hadronic interaction with the Solar nuclei, leading to a low-energy neutrino flux. The low density in the solar atmosphere allows those mesons to propagate long distances without any interaction, which contributes to generating a large neutrino flux at high energies.

While many attempts have been made to calculate this flux since it was first proposed, there is still uncertainties on the flux arising from a variety of factors. For instance, the primary cosmic-ray model, solar density model, and hadronic interaction modify the initial spectrum of neutrinos, while uncertainties on the neutrino oscillation parameters alter the propagated spectrum. Additionally, uncertainties on the interactions of charged mesons and cosmic rays with the solar magnetic field have a large impact on the flux, especially at lower energies. In addition to these uncertainties, there is disagreement on the overall normalization at the level of a factor of ~ 2 between calculations.

In Fig. 2, we show three recent calculations of the solar atmospheric neutrino flux after

propagation from the point of creation to the Earth's surface from [5–7]. Each calculation includes different uncertainties, which are shown as the shaded regions. For example, the calculations shown in red and purple both include uncertainties due to the primary cosmic-ray model, with the calculation in red additionally including the effect uncertainties on the hadronic interaction model and neutrino oscillation parameters. The calculation shown in blue includes the uncertainty on the solar magnetic field.

In Fig. 2, we also show the nominal model used in this work as a black, dashed line, taken from Argüelles, *et al.* [5]. This model uses the Hillas-Gaisser H4a as the cosmic-ray model and SIBYLL-2.3 as the hadronic model. In Sec. 5, we give our sensitivity in terms of a normalization on this model; however, we note that, since the effect of the shapes is subdominant in this analysis, sensitivities to other models can be achieved by taking the ratio of the integrated fluxes.

3. The IceCube Neutrino Observatory

IceCube is a cubic-kilometer-scale neutrino telescope deployed in the ice beneath the geographic South Pole [8]. Over 5000 digital optical modules (DOMs) detect the Cherenkov radiation emitted after neutrinos interact and create charged particle in or near the the detector. These DOMs are deployed at depths ranging from 1450 m to 2450 m beneath the surface. The primary component of the detector is comprised of 78 strings with a horizontal separation of $\sim$ 125 m and a vertical separation of 17 m between DOMs. This inter-DOM spacing allows for the efficient detection of neutrinos with energies from 100 GeV to 10^8 GeV. Additionally, there are eight additional more densely packed strings in the center of the detector. In this region, known as the DeepCore subarray, the DOMs are vertically separated by 7 m–10 m. This allows for the detection of neutrinos with energies as low as a few GeV.

In IceCube, events are usually classified into two different *event morphologies*. *Tracks*, are long, line-like events that are generated as a $\mu^{\pm}$ from a ν_{μ} charged-current interaction travels through the ice, and *cascades* are spherical events produced by ν_e and ν_{τ} charged-current interactions or by ν_{α} neutral-current interactions. Since at energies above $\sim$ 500 GeV, μ can travel $\gtrsim$ 1 km, track events have good angular resolution—$\Delta\theta < 1°$) [9]—and thus, should be useful when looking for a signal from the direction of the Sun. While the angular construction of cascade events is more challenging, they may still provide some power in our analysis. At the lowest energies directional reconstruction is difficult for all events, and since neutrino oscillations increase the relative number of cascades in the solar atmospheric flux, including cascades may add to sensitivity.

4. Event selection

Previous searches focus in tracks with energies above the TeV scale. In this analysis, we want to extend the search to lower energy covering the whole energy range to which IceCube is sensitive. For the high energies, we use the northern-sky high-energy track selection [10], which provide a good pointing resolution. This selection consider events with a reconstruction neutrino zenith angle larger than $\theta_{\nu}^{\text{reco}} > 85$. The final analysis variables are the reconstructed neutrino energy and the angular distance from the center of the Sun. Since the Sun is not at a fixed point in the sky, this latter quantity depends on the time of the event and the reconstructed neutrino direction. The angular
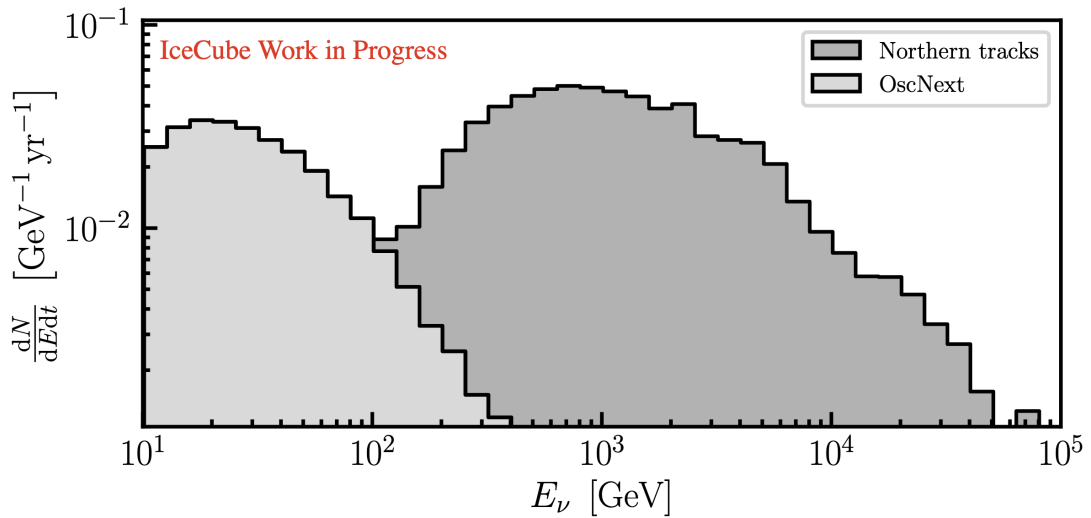
Figure 3: *Event distribution in the OscNext and northern track event selections.* Both distribution peaks at ~ 20 GeV and ~ 1 TeV. For energies between 50 GeV and 300 GeV, there is an gap in the event rate due to the lack of event selection targeting that energy region. One of the goal of this analysis is to create a medium-energy event selection.

reconstruction is performed by branched decision tree and the reconstructed energy it is based on a deep neural network.

For low energy, we use IceCube's next generation low-energy oscillation event selection [11], and contains events from all-flavors charged- and neutral currents. This analysis consider the lowest energy events that IceCube is sensitive, from ~ 6 GeV to 100 GeV. To avoid any interference with the other sample, we remove all the events passing the *MuonFilter*, which select the events where the number of hit DOMs is larger than 8 for the up-going events, as it is the requisites to enter in the high energy selection.

In Figure 3, we can see the event distribution for the low- and high-energy event selections as a function of the neutrino energy. OscNext and northern tracks covers the neutrino distribution for $E_\nu < 50$ GeV and $E_\nu > 700$ GeV. For energies between those two ranges, the selection criteria used by these to samples lead to gap in the sample, as shown in Figure 3. The goal of this analysis is the development of an event selection that targets the energy region between the low- and the high-energy event selections. To do that, we are considering the low energy events in the full IceCube instrumented volume that passes the LowUp filter, which selects the low-energy up-going events in IceCube. In this sample, all the events triggered by the LowUp filter are also removed. After designing optimize cuts over the reconstructed vertex ($COG_{x,y,z}$), the uncertainty in the location of the vertex (σ_{COG}), the distance travelled in the vertical direction (Z_{travel}), and the reconstructed zenith (θ_{reco}) to maximize the relative gain in significance, we are developing a booster decision tree (BDT) that allow us to reduce the rate of atmospheric muons in the selection.
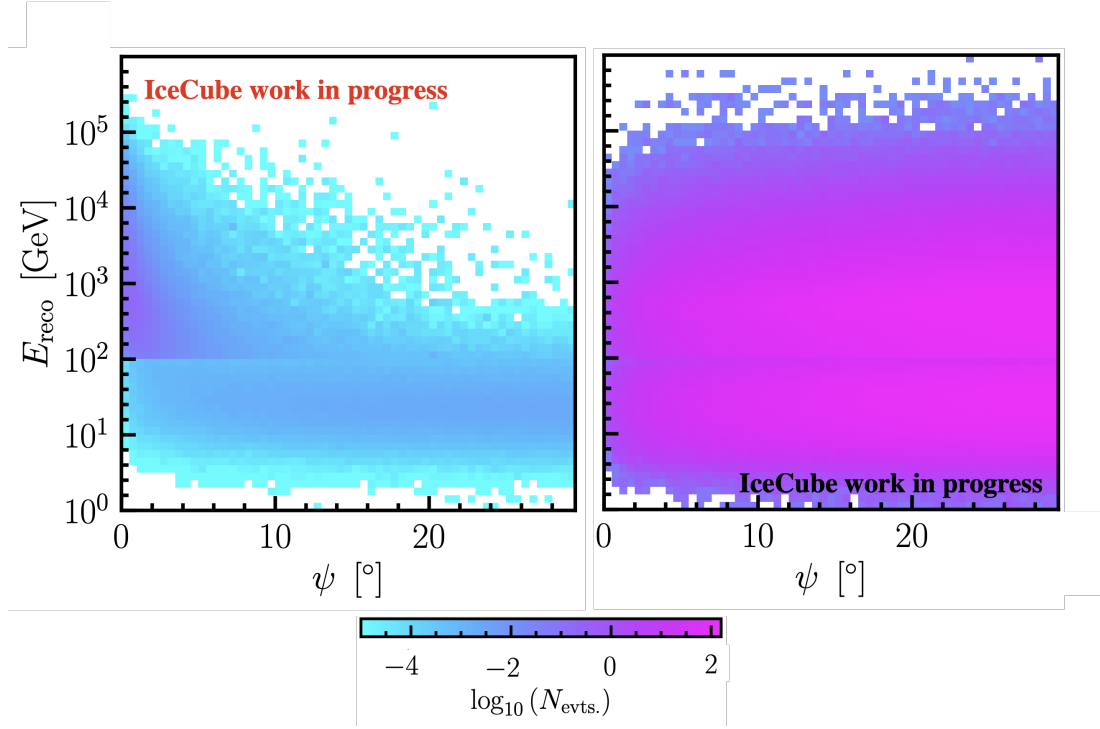
Figure 4: *Combined analysis-level event distributions for high-energy and low-energy selections.* The left plot shows the event distribution for the nominal signal model, while the right plot shows the data-driven background distribution. All events in the left plot originate from the Sun, *i.e.* at $\psi = 0$, and the purple region is evidence of the improved angular resolution of the high-energy track selection. Note also the faint line one can see at ~ 100 GeV in the right plot, which is the manifestation of the energy gap in reconstructed variables.

5. Statistical Treatment and Sensitivity

For this analysis, we do a binned likelihood. In the low- and high-energy selections, we bin logarithmically in the reconstructed energy, and linearly in the reconstructed angular distance from the enter of the Sun, as seen in Fig. 4. Additionally, we split the low-energy selection into three bins dictated by a BDT score that separates tracks and cascades.

We use the Poisson likelihood for this analysis, *i.e.* the likelihood is given by:

$$\mathcal{L}(\vec{\theta}|n) = \prod_i \frac{e^{-\mu_i} \mu_i^{n_i}}{n_i!},$$

where $\vec{\theta}$ are the model parameters, n is the observed data, i indexes the bin, μ_i is the expected number of events from a given model in the ith bin, and n_i is the observed number of events in the ith bin. We then define the log-likelihood, LLH as:

$$\ln \mathcal{L} = \ln \left[\prod_i \frac{e^{-\mu_i} \mu_i^{n_i}}{n_i!} \right] = \sum_i -\mu_i + n_i \ln \mu_i - \ln n_i!.$$

We may optimize over the model parameters, $\vec{\theta}$, in order to find the model which best describes the observed data. In this analysis, these model parameters are the normalizations of the nominal
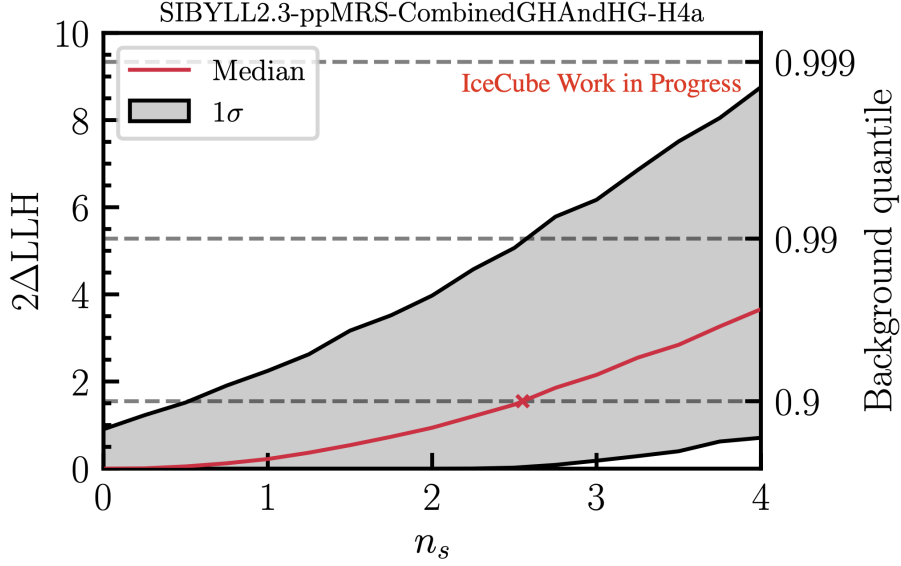
Figure 5: *Median and 1σ test-statistics as a function of the injected signal normalization.* The red line gives the median test statistic for 10,000 pseudoëxperiments at each normalization. The gray band shows the 1σ range for the same set of pseudoëxperiments. Horizontal, gray dashed lines indicate the positions of certain background quantiles test-statistic values. We mark the point where we achieve our median 90% sensitivity with a red "x."

signal and background distributions, *i.e.* $\vec{\theta} = \langle n_s, n_b \rangle$, and the model is given by

$$\mu = n_s \, \mu_s + n_b \, \mu_b.$$

We construct our sensitivity from trials for this analysis. To do this, we consider a model given by a set of model parameters, $\vec{\theta}^{\text{true}} = \langle n_s^{\text{true}}, 1 \rangle$, where we have set the background normalization to 1 since the background is derived from data. We then draw data realizations, *i.e.* for each bin, we draw a number, n_i, from a Poisson distribution with a mean $\lambda = n_s \mu_{s,i} + \mu_{b,i}$. We then fit then maximize the likelihood under two different model assumptions: $\hat{\theta}_s = \langle \hat{n}_s, \hat{n}_b \rangle$ and $\hat{\theta}_b = \langle 0, \hat{\hat{n}}_b \rangle$, called the signal-plus-background model, and the background-only model respectively. We then define our test statistic as:

$$\text{TS} = 2 \left[\ln \mathcal{L}(\hat{\theta}_s | n) - \ln \mathcal{L}(\hat{\theta}_b | n) \right].$$

Simply put, this quantifies the degree to which the signal-plus-background model better the data than the background-only model. By repeating this procedure a number of times, we build a *test-statistic* distribution for a particular model.

We then define our median sensitivity at q confidence, as the model whose test-statistic distribution has a median value that is greater than $q\%$ of the background test-statistic distribution. In words, this means that if this model were the true model, we would be able to reject the background-only model at with a p-value of $p = 1 - q/100$ half the time. We should note that this is a slightly different definition of sensitivity than that typically used by IceCube point source searches, in which the sensitivity is defined as the model at which 90% of test-statistics exceed the median of the background test-statistic distribution. We believe that the definition we have chosen lends

7

itself to a cleaner statistical interpretation and is more in line with the colloquial understanding of the word "sensitivity." We find that using only the northern tracks selection, we have sensitivity to 2.55 times our nominal model. We also find that if the true model is the nominal model, we should expect to be able to see it at 95% confidence 14% of the time. See Fig 5 for a visual representation of this information. This sensitivty is comparable to a complimentary IceCube search for solar atmospheric neutrinos [12]

6. Conclusion

In this proceeding, we have shown the current status of an on-going search for solar atmospheric neutrinos with the IceCube Neutrino Observatory. This analysis aims to use neutrinos over the whole energy range to which IceCube is sensitive. To do this we are combining existing low- and high-energy selections with a new medium-energy selection. Using only the high- and low-energy selections, we show a sensitivity to 2.55x the nominal model considered in this paper. Additionally, we should that there is a chance of observing the nominal model at 95% confidence 15% of the time.

References

[1] **BOREXINO** Collaboration, S. Appel *et al.* *Phys. Rev. Lett.* **129** no. 25, (2022) 252701.

[2] R. Davis, Jr., D. S. Harmer, and K. C. Hoffman *Phys. Rev. Lett.* **20** (1968) 1205–1209.

[3] **Fermi-LAT** Collaboration, A. A. Abdo *et al.* *The Astrophysical Journal* **734** no. 2, (Jun, 2011) 116.

[4] **HAWC** Collaboration, A. Albert *et al.* arXiv:2212.00815.

[5] C. A. Argüelles, G. de Wasseige, A. Fedynitch, and B. J. P. Jones *JCAP* **07** (2017) 024.

[6] K. C. Y. Ng, J. F. Beacom, A. H. G. Peter, and C. Rott *Phys. Rev. D* **96** no. 10, (2017) 103006.

[7] J. Edsjo, J. Elevant, R. Enberg, and C. Niblaeus *JCAP* **06** (2017) 033.

[8] **IceCube** Collaboration, A. Achterberg *et al.* *Astropart. Phys.* **26** (2006) 155–173.

[9] **IceCube** Collaboration, M. G. Aartsen *et al.* *Astrophys. J.* **835** no. 2, (2017) 151.

[10] **IceCube** Collaboration, R. Abbasi *et al.* *Science* **378** no. 6619, (2022) 538–543.

[11] **IceCube** Collaboration, R. Abbasi *et al.* arXiv:2304.12236.

[12] G. Roellinghoff, *Search for Solar Atmospheric Neutrinos using 9 years of IceCube Neutrino Detector data.* PhD thesis, Sungkyunkwan University, 2022.

Full Author List: IceCube Collaboration

R. Abbasi[17], M. Ackermann[63], J. Adams[18], S. K. Agarwalla[40, 64], J. A. Aguilar[12], M. Ahlers[22], J.M. Alameddine[23], N. M. Amin[44], K. Andeen[42], G. Anton[26], C. Argüelles[14], Y. Ashida[53], S. Athanasiadou[63], S. N. Axani[44], X. Bai[50], A. Balagopal V.[40], M. Baricevic[40], S. W. Barwick[30], V. Basu[40], R. Bay[8], J. J. Beatty[20, 21], J. Becker Tjus[11, 65], J. Beise[61], C. Bellenghi[27], C. Benning[1], S. BenZvi[52], D. Berley[19], E. Bernardini[48], D. Z. Besson[36], E. Blaufuss[19], S. Blot[63], F. Bontempo[31], J. Y. Book[14], C. Boscolo Meneguolo[48], S. Böser[41], O. Botner[61], J. Böttcher[1], E. Bourbeau[22], J. Braun[40], B. Brinson[6], J. Brostean-Kaiser[63], R. T. Burley[2], R. S. Busse[43], D. Butterfield[40], M. A. Campana[49], K. Carloni[14], E. G. Carnie-Bronca[2], S. Chattopadhyay[40, 64], N. Chau[12], C. Chen[6], Z. Chen[55], D. Chirkin[40], S. Choi[56], B. A. Clark[19], L. Classen[43], A. Coleman[61], G. H. Collin[15], A. Connolly[20, 21], J. M. Conrad[15], P. Coppin[13], P. Correa[13], D. F. Cowen[59, 60], P. Dave[6], C. De Clercq[13], J. J. DeLaunay[58], D. Delgado[14], S. Deng[1], K. Deoskar[54], A. Desai[40], P. Desiati[40], K. D. de Vries[13], G. de Wasseige[37], T. DeYoung[24], A. Diaz[15], J. C. Díaz-Vélez[40], M. Dittmer[43], A. Domi[26], H. Dujmovic[40], M. A. DuVernois[40], T. Ehrhardt[41], P. Eller[27], E. Ellinger[62], S. El Mentawi[1], D. Elsässer[23], R. Engel[31, 32], H. Erpenbeck[40], J. Evans[19], P. A. Evenson[44], K. L. Fan[19], K. Fang[40], K. Farrag[16], A. R. Fazely[7], A. Fedynitch[57], N. Feigl[10], S. Fiedlschuster[26], C. Finley[54], L. Fischer[63], D. Fox[59], A. Franckowiak[11], A. Fritz[41], P. Fürst[1], J. Gallagher[39], E. Ganster[1], A. Garcia[14], L. Gerhardt[9], A. Ghadimi[58], C. Glaser[61], T. Glauch[27], T. Glüsenkamp[26, 61], N. Goehlke[32], J. G. Gonzalez[44], S. Goswami[58], D. Grant[24], S. J. Gray[19], O. Gries[1], S. Griffin[40], S. Griswold[52], K. M. Groth[22], C. Günther[1], P. Gutjahr[23], C. Haack[26], A. Hallgren[61], R. Halliday[24], L. Halve[1], F. Halzen[40], H. Hamdaoui[55], M. Ha Minh[27], K. Hanson[40], J. Hardin[15], A. A. Harnisch[24], P. Hatch[33], A. Haungs[31], K. Helbing[62], J. Hellrung[11], F. Henningsen[27], L. Heuermann[1], N. Heyer[61], S. Hickford[62], A. Hidvegi[54], C. Hill[16], G. C. Hill[2], K. D. Hoffman[19], S. Hori[40], K. Hoshina[40, 66], W. Hou[31], T. Huber[31], K. Hultqvist[54], M. Hünnefeld[23], R. Hussain[40], K. Hymon[23], S. In[56], A. Ishihara[16], M. Jacquart[40], O. Janik[1], M. Jansson[54], G. S. Japaridze[5], M. Jeong[56], M. Jin[14], B. J. P. Jones[4], D. Kang[31], W. Kang[56], X. Kang[49], A. Kappes[43], D. Kappesser[41], L. Kardum[23], T. Karg[63], M. Karl[27], A. Karle[40], U. Katz[26], M. Kauer[40], J. L. Kelley[40], A. Khatee Zathul[40], A. Kheirandish[34, 35], J. Kiryluk[55], S. R. Klein[8, 9], A. Kochocki[24], R. Koirala[44], H. Kolanoski[10], T. Kontrimas[27], L. Köpke[41], C. Kopper[26], D. J. Koskinen[22], P. Koundal[31], M. Kovacevich[49], M. Kowalski[10, 63], T. Kozynets[22], J. Krishnamoorthi[40, 64], K. Kruiswijk[37], E. Krupczak[24], A. Kumar[63], E. Kun[11], N. Kurahashi[49], N. Lad[63], C. Lagunas Gualda[63], M. Lamoureux[37], M. J. Larson[19], S. Latseva[1], F. Lauber[62], J. P. Lazar[14, 40], J. W. Lee[56], K. Leonard DeHolton[60], A. Leszczyńska[44], M. Lincetto[11], Q. R. Liu[40], M. Liubarska[25], E. Lohfink[41], C. Love[49], C. J. Lozano Mariscal[43], L. Lu[40], F. Lucarelli[28], W. Luszczak[20, 21], Y. Lyu[8, 9], J. Madsen[40], K. B. M. Mahn[24], Y. Makino[40], E. Manao[27], S. Mancina[40, 48], W. Marie Sainte[40], I. C. Mariş[12], S. Marka[46], Z. Marka[46], M. Marsee[58], I. Martinez-Soler[14], R. Maruyama[45], F. Mayhew[24], T. McElroy[25], F. McNally[38], J. V. Mead[22], K. Meagher[40], S. Mechbal[63], A. Medina[21], M. Meier[16], Y. Merckx[13], L. Merten[11], J. Micallef[24], J. Mitchell[7], T. Montaruli[28], R. W. Moore[25], Y. Morii[16], R. Morse[40], M. Moulai[40], T. Mukherjee[31], R. Naab[63], R. Nagai[16], M. Nakos[40], U. Naumann[62], J. Necker[63], A. Negi[4], M. Neumann[43], H. Niederhausen[24], M. U. Nisa[24], A. Noell[1], A. Novikov[44], S. C. Nowicki[24], A. Obertacke Pollmann[16], V. O'Dell[40], M. Oehler[31], B. Oeyen[29], A. Olivas[19], R. Ørsøe[27], J. Osborn[40], E. O'Sullivan[61], H. Pandya[44], N. Park[33], G. K. Parker[4], E. N. Paudel[44], L. Paul[42, 50], C. Pérez de los Heros[61], J. Peterson[40], S. Philippen[1], A. Pizzuto[40], M. Plum[50], A. Pontén[61], Y. Popovych[41], M. Prado Rodriguez[40], B. Pries[24], R. Procter-Murphy[19], G. T. Przybylski[9], C. Raab[37], J. Rack-Helleis[41], K. Rawlins[3], Z. Rechav[40], A. Rehman[44], P. Reichherzer[11], G. Renzi[12], E. Resconi[27], S. Reusch[63], W. Rhode[23], B. Riedel[40], A. Rifaie[1], E. J. Roberts[2], S. Robertson[8, 9], S. Rodan[56], G. Roellinghoff[56], M. Rongen[26], C. Rott[53, 56], T. Ruhe[23], L. Ruohan[27], D. Ryckbosch[29], I. Safa[14, 40], J. Saffer[32], D. Salazar-Gallegos[24], P. Sampathkumar[31], S. E. Sanchez Herrera[24], A. Sandrock[62], M. Santander[58], S. Sarkar[25], S. Sarkar[47], J. Savelberg[1], P. Savina[40], M. Schaufel[1], H. Schieler[31], S. Schindler[26], L. Schlickmann[1], B. Schlüter[43], F. Schlüter[12], N. Schmeisser[62], T. Schmidt[19], J. Schneider[26], F. G. Schröder[31, 44], L. Schumacher[26], G. Schwefer[1], S. Sclafani[19], D. Seckel[44], M. Seikh[36], S. Seunarine[51], R. Shah[49], A. Sharma[61], S. Shefali[32], N. Shimizu[16], M. Silva[40], B. Skrzypek[14], B. Smithers[4], R. Snihur[40], J. Soedingrekso[23], A. Søgaard[22], D. Soldin[32], P. Soldin[1], G. Sommani[11], C. Spannfellner[27], G. M. Spiczak[51], C. Spiering[63], M. Stamatikos[21], T. Stanev[44], T. Stezelberger[9], T. Stürwald[62], T. Stuttard[22], G. W. Sullivan[19], I. Taboada[6], S. Ter-Antonyan[7], M. Thiesmeyer[1], W. G. Thompson[14], J. Thwaites[40], S. Tilav[44], K. Tollefson[24], C. Tönnis[56], S. Toscano[12], D. Tosi[40], A. Trettin[63], C. F. Tung[6], R. Turcotte[31], J. P. Twagirayezu[24], B. Ty[40], M. A. Unland Elorrieta[43], A. K. Upadhyay[40, 64], K. Upshaw[7], N. Valtonen-Mattila[61], J. Vandenbroucke[40], N. van Eijndhoven[13], D. Vannerom[15], J. van Santen[63], J. Vara[43], J. Veitch-Michaelis[40], M. Venugopal[31], M. Vereecken[37], S. Verpoest[44], D. Veske[46], A. Vijai[19], C. Walck[54], C. Weaver[24], P. Weigel[15], A. Weindl[31], J. Weldert[60], C. Wendt[40], J. Werthebach[23], M. Weyrauch[31], N. Whitehorn[24], C. H. Wiebusch[1], N. Willey[24], D. R. Williams[58], L. Witthaus[23], A. Wolf[1], M. Wolf[27], G. Wrede[26], X. W. Xu[7], J. P. Yanez[25], E. Yildizci[40], S. Yoshida[16], R. Young[36], F. Yu[14], S. Yu[24], T. Yuan[40], Z. Zhang[55], P. Zhelnin[14], M. Zimmerman[40]

[1] III. Physikalisches Institut, RWTH Aachen University, D-52056 Aachen, Germany
[2] Department of Physics, University of Adelaide, Adelaide, 5005, Australia
[3] Dept. of Physics and Astronomy, University of Alaska Anchorage, 3211 Providence Dr., Anchorage, AK 99508, USA
[4] Dept. of Physics, University of Texas at Arlington, 502 Yates St., Science Hall Rm 108, Box 19059, Arlington, TX 76019, USA
[5] CTSPS, Clark-Atlanta University, Atlanta, GA 30314, USA
[6] School of Physics and Center for Relativistic Astrophysics, Georgia Institute of Technology, Atlanta, GA 30332, USA
[7] Dept. of Physics, Southern University, Baton Rouge, LA 70813, USA
[8] Dept. of Physics, University of California, Berkeley, CA 94720, USA
[9] Lawrence Berkeley National Laboratory, Berkeley, CA 94720, USA
[10] Institut für Physik, Humboldt-Universität zu Berlin, D-12489 Berlin, Germany
[11] Fakultät für Physik & Astronomie, Ruhr-Universität Bochum, D-44780 Bochum, Germany
[12] Université Libre de Bruxelles, Science Faculty CP230, B-1050 Brussels, Belgium

[13] Vrije Universiteit Brussel (VUB), Dienst ELEM, B-1050 Brussels, Belgium
[14] Department of Physics and Laboratory for Particle Physics and Cosmology, Harvard University, Cambridge, MA 02138, USA
[15] Dept. of Physics, Massachusetts Institute of Technology, Cambridge, MA 02139, USA
[16] Dept. of Physics and The International Center for Hadron Astrophysics, Chiba University, Chiba 263-8522, Japan
[17] Department of Physics, Loyola University Chicago, Chicago, IL 60660, USA
[18] Dept. of Physics, University of Canterbury, Private Bag 4800, Christchurch, New Zealand
[19] Dept. of Physics, University of Maryland, College Park, MD 20742, USA
[20] Dept. of Astronomy, Ohio State University, Columbus, OH 43210, USA
[21] Dept. of Physics and Center for Cosmology and Astro-Particle Physics, Ohio State University, Columbus, OH 43210, USA
[22] Niels Bohr Institute, University of Copenhagen, DK-2100 Copenhagen, Denmark
[23] Dept. of Physics, TU Dortmund University, D-44221 Dortmund, Germany
[24] Dept. of Physics and Astronomy, Michigan State University, East Lansing, MI 48824, USA
[25] Dept. of Physics, University of Alberta, Edmonton, Alberta, Canada T6G 2E1
[26] Erlangen Centre for Astroparticle Physics, Friedrich-Alexander-Universität Erlangen-Nürnberg, D-91058 Erlangen, Germany
[27] Technical University of Munich, TUM School of Natural Sciences, Department of Physics, D-85748 Garching bei München, Germany
[28] Département de physique nucléaire et corpusculaire, Université de Genève, CH-1211 Genève, Switzerland
[29] Dept. of Physics and Astronomy, University of Gent, B-9000 Gent, Belgium
[30] Dept. of Physics and Astronomy, University of California, Irvine, CA 92697, USA
[31] Karlsruhe Institute of Technology, Institute for Astroparticle Physics, D-76021 Karlsruhe, Germany
[32] Karlsruhe Institute of Technology, Institute of Experimental Particle Physics, D-76021 Karlsruhe, Germany
[33] Dept. of Physics, Engineering Physics, and Astronomy, Queen's University, Kingston, ON K7L 3N6, Canada
[34] Department of Physics & Astronomy, University of Nevada, Las Vegas, NV, 89154, USA
[35] Nevada Center for Astrophysics, University of Nevada, Las Vegas, NV 89154, USA
[36] Dept. of Physics and Astronomy, University of Kansas, Lawrence, KS 66045, USA
[37] Centre for Cosmology, Particle Physics and Phenomenology - CP3, Université catholique de Louvain, Louvain-la-Neuve, Belgium
[38] Department of Physics, Mercer University, Macon, GA 31207-0001, USA
[39] Dept. of Astronomy, University of Wisconsin–Madison, Madison, WI 53706, USA
[40] Dept. of Physics and Wisconsin IceCube Particle Astrophysics Center, University of Wisconsin–Madison, Madison, WI 53706, USA
[41] Institute of Physics, University of Mainz, Staudinger Weg 7, D-55099 Mainz, Germany
[42] Department of Physics, Marquette University, Milwaukee, WI, 53201, USA
[43] Institut für Kernphysik, Westfälische Wilhelms-Universität Münster, D-48149 Münster, Germany
[44] Bartol Research Institute and Dept. of Physics and Astronomy, University of Delaware, Newark, DE 19716, USA
[45] Dept. of Physics, Yale University, New Haven, CT 06520, USA
[46] Columbia Astrophysics and Nevis Laboratories, Columbia University, New York, NY 10027, USA
[47] Dept. of Physics, University of Oxford, Parks Road, Oxford OX1 3PU, United Kingdom
[48] Dipartimento di Fisica e Astronomia Galileo Galilei, Università Degli Studi di Padova, 35122 Padova PD, Italy
[49] Dept. of Physics, Drexel University, 3141 Chestnut Street, Philadelphia, PA 19104, USA
[50] Physics Department, South Dakota School of Mines and Technology, Rapid City, SD 57701, USA
[51] Dept. of Physics, University of Wisconsin, River Falls, WI 54022, USA
[52] Dept. of Physics and Astronomy, University of Rochester, Rochester, NY 14627, USA
[53] Department of Physics and Astronomy, University of Utah, Salt Lake City, UT 84112, USA
[54] Oskar Klein Centre and Dept. of Physics, Stockholm University, SE-10691 Stockholm, Sweden
[55] Dept. of Physics and Astronomy, Stony Brook University, Stony Brook, NY 11794-3800, USA
[56] Dept. of Physics, Sungkyunkwan University, Suwon 16419, Korea
[57] Institute of Physics, Academia Sinica, Taipei, 11529, Taiwan
[58] Dept. of Physics and Astronomy, University of Alabama, Tuscaloosa, AL 35487, USA
[59] Dept. of Astronomy and Astrophysics, Pennsylvania State University, University Park, PA 16802, USA
[60] Dept. of Physics, Pennsylvania State University, University Park, PA 16802, USA
[61] Dept. of Physics and Astronomy, Uppsala University, Box 516, S-75120 Uppsala, Sweden
[62] Dept. of Physics, University of Wuppertal, D-42119 Wuppertal, Germany
[63] Deutsches Elektronen-Synchrotron DESY, Platanenallee 6, 15738 Zeuthen, Germany
[64] Institute of Physics, Sachivalaya Marg, Sainik School Post, Bhubaneswar 751005, India
[65] Department of Space, Earth and Environment, Chalmers University of Technology, 412 96 Gothenburg, Sweden
[66] Earthquake Research Institute, University of Tokyo, Bunkyo, Tokyo 113-0032, Japan

Acknowledgements

PoS(ICRC2023)1116